Available online at www.sciencedirect.com

ScienceDirect

journal homepage: www.elsevier.com/locate/issn/15375110

Special Issue: Irrigated Agriculture

Research Paper

Detecting crop water status in mature olive groves using vegetation spectral measurements

Giovanni Rallo [a], *Mario Minacapilli* [a,*], *Giuseppe Ciraolo* [b], *Giuseppe Provenzano* [a]

[a] *Department of Agricultural and Forest Sciences (SAF), Università degli Studi di Palermo, Viale delle Scienze Ed. 4, 90128, Palermo, Italy*

[b] *Department of Civil, Environmental and Aerospace Engineering (DICAM), Università degli Studi di Palermo, Viale delle Scienze Ed. 8, 90128, Palermo, Italy*

ARTICLE INFO

Article history:
Published online 15 September 2014

Keywords:
Spectroscopy
Leaf water potential
Crop water status
Olive tree

Full spectral measurements (350–2500 nm) at tree canopy and leaf levels and the corresponding leaf water potentials (LWP) were acquired in an olive grove of Sicily, at different hours of the day, during summer season 2011. The main objective of the work was to assess, on the basis of the experimental data-set, two different approaches to detect crop water status in terms of LWP. Specifically, using existing families of Vegetation Indices (VIs) and applying Partial Least Squares Regression (PLSR) were optimised and tested. The results indicated that a satisfactory estimation of LWP at tree canopy and leaf levels can be obtained using vegetation indices based on the near infrared–shortwave infrared (NIR–SWIR) domain requiring, however, a specific optimisation of the corresponding "centre-bands". At tree canopy level, a good prediction of LWP was obtained by using optimised indices working in the visible domain, like the Normalized Difference Greenness Vegetation Index (NDGI, RMSE = 0.37 and R^2 = 0.57), the Green Index (GI, RMSE = 0.53 and R^2 = 0.39) and the Moisture Spectral Index (MSI, RMSE = 0.41 and R^2 = 0.48). On the other hand, a satisfactory estimation of LWP at leaf level was obtained using indices combining SWIR and NIR wavelengths. The best prediction was specifically found by optimising the MSI (RMSE of 0.72 and R^2 = 0.45) and the Normalized Difference Water Index (NDWI, RMSE = 0.75 and R^2 = 0.45). Even using the PLSR technique, a remarkable prediction of LWP at both tree canopy and leaf levels was obtained. However, this technique requires the availability of full spectra with high resolution, which can only be obtained with handheld spectroradiometers or hyper-spectral remote sensors.

* *Corresponding author*. Tel.: +39 (0)91 23897075; fax: +39 (0)91 484035.
E-mail address: mario.minacapilli@unipa.it (M. Minacapilli).

http://dx.doi.org/10.1016/j.biosystemseng.2014.08.012
1537-5110/

1. Introduction

In typical Mediterranean agro-ecosystems, characterised by long dry seasons and limited water resources, soil-plant water deficit is the main environmental constraint on crop yield. In the last decades, the growing demand for olive tree products has suggested the need to use a precise irrigation scheduling accounting for soil and/or crop water status (Provenzano, Tarquis, & Rodriguez-Sinobas, 2013). Particularly, leaf water potential (LWP) is considered one of the most reliable indicators of crop water status and it can be used as an irrigation scheduling parameter (Jones, 2004). Over large areas, measurements of LWP are labour-intensive and time-consuming, due to the large number of observations necessary to characterise a single plot. As a consequence, non-destructive and fast methodologies to assess crop water status or other related parameters are desirable. In this context, reflectance spectroscopy in the electromagnetic regions of visible (VIS), near infrared (NIR) and shortwave infrared (SWIR) can be applied for indirect evaluations of crop water status across various spatial scales (Gamon & Qiu, 1999).

The theoretical base that justifies the use of spectroradiometric techniques refers to the direct interactions between the VIS, NIR and SWIR vegetation spectral signatures and physiological parameters, photosynthetic activity (Gamon, Serrano, & Surfus, 1997) and leaf water status (Elsayed, Mistele, & Schmidhalter, 2011). In fact, changes in leaf internal structure due to reduced water contents influence reflectance in the red and near infrared spectral regions (Inoue, Morinaga, & Shibayama, 1993). In NIR and SWIR regions, several water spectral absorption bands near 970, 1200, 1450, and 1940 nm can be used to detect crop water status (Curran, 1989). Peñuelas, Filella, Biel, Serrano, & Savé, 1993, Penuelas, Gamon, Fredeen, Merino, and Field (1994), studying the reflectance signature of gerbera, pepper, bean plants and wheat in the NIR domain, proposed the ratio of reflectance at 970 and 900 nm, in order to evaluate a Water Index, WI, to monitor the changes in relative water content, leaf water potential, stomatal conductance, and cell wall elasticity. Tian, Tong, Pu, Guo, and Zhao (2001) obtained a high prediction accuracy for wheat water content from spectral absorption features between 1650 and 1850 nm. In addition, the use of reflectance spectroscopy in the visible region provides information that can be associated with pigments like chlorophyll, carotenoids, anthocyanin and consequently to photosynthetic processes of leaves (Sims & Gamon, 2002), indirectly related to leaf/plant water status.

Another distinctive feature of reflectance spectroscopy is its applicability across various spatial scales, from leaf and tree canopy level, using standard handheld spectroradiometers, to higher levels by means of multispectral and hyperspectral remote sensing technologies. In the past decades, many relationships between spectral data from remote sensing observations and various biophysical and physiological crops parameters (leaf area index, leaf greenness, leaf chlorophyll content, etc.) have been proposed (Liang, 2004, chap. 3). A common and widely used approach to analyse crop spectral signatures acquired from remote sensing platforms is based on the extraction of so-called Vegetation Indices (VIs). These indices can be obtained from multispectral systems able to capture images in a few "broad" spectral bands (with spectral resolution of about 50 nm), usually centred in VIS–NIR regions. For example, the Normalized Difference Vegetation Index (NDVI), based on a simple combination of reflectance values in visible (red or green) and near-infrared regions, has been widely used to map, at various observation scales, crop variables like biomass, Leaf Area Index (LAI), plant coverage and chlorophyll (Aparicio, Villegas, Casadesus, Araus, & Royo, 2000; Christensen & Goudriaan, 1993). Moreover, NDVI or other similar VIs, using average spectral information, have been used to assess the spatial variability of crop variables over large areas (Myneni, Los, & Asrar, 1995; Tucker, Fung, Keeling, & Gammon, 1986). However, this kind of information has to be properly used in order to consider the same observation scale for both VIs and the investigated crop properties. Recently, Marino et al. (2014) collected a large dataset of diurnal and seasonal measurements of leaf gas exchange and plant transpiration, highlighting that the Photochemical Reflectance Index (PRI) and the Water Index (WI), measured at the tree canopy, can be used to detect water stress. However, these authors only considered three indices of the VIS–NIR family, without including the SWIR region.

The recent technological progress in the industrial production of handheld spectroradiometers and hyperspectral sensors, characterised by a high number of contiguous spectral bands (resolution better than 10 nm), has driven scientists to a more accurate analysis aimed at selecting specific wavebands that should be more sensitive to crop-related variables (Blackburn, 1998; Darvishzadeh et al., 2008; Goel, Prasher, Landry, Patel, & Viau, 2003; Maccioni, Agat, & Mazzinghi, 2001). For example, using hyperspectral imagery, Zarco-Tejada et al. (2013) demonstrated the ability of a VI, centred at 570 and 515 nm wavelengths, to assess carotenoid content at canopy level and proposed a new formulation of the PRI, centred at 531 and 570 nm wavelengths, as a water stress indicator.

Moreover, various studies have considered the full spectral information on the basis of multivariate statistical techniques, e.g. Partial Least Squares Regression (PLSR), to take advantages of an increased number of wavebands, to improve the prediction of crop related parameters (Esbensen, 2000, 598 pp.; Hansen & Schjoerring, 2003). However, little research has combined leaf and canopy spectral measurements to assess crop water stress and to exploit the link between physical variables and spectral measurements. Recently, a specific database, containing more than 30 different indices related to "vegetation – water" applications, has been published on-line by the Institute of Crop Science and Resource Conservation (INRES, www.indexdatabase.de) of Bonn University. Unfortunately, the proposed indices are not related to any specific crop or to physical variables. Despite the growing interest in the research topic, demonstrated by the copious literature, only a limited number of investigations have considered the spectral behaviour of Mediterranean crops, like olives, across various scales.

In this context, in the frame of a rational recognition of VIS–NIR and SWIR spectroradiometric techniques, useful to characterise water status of olive crop, the specific objectives of the paper are: i) to assess relation of leaf water potentials (LWP) of a Mediterranean olive grove to high spectral resolution reflectance, in order to optimise a set of VI families that could be used at leaf or tree canopy level for a fast and non-destructive detection of water status; ii) to test a classic multivariate analysis (PLSR), using the full spectral measurements in the VIS–SWIR regions, in order to improve LWP prediction accuracy.

2. Materials and methods

2.1. Study area and experimental design

Experiments were carried out at "Tenuta Rocchetta", a commercial farm located near Castelvetrano, Sicily (Lat: 37° 38′ 35″N; Lon: 12° 50′ 50″E), in a territory where olive (*Olea europaea* L., cv Nocellara del Belice) is the dominant crop. Experiments were carried out on 15 year old olive trees, planted on a regular grid of 8 × 5 m^2 (250 trees per hectare), characterised by a trunk cross sectional area of about 320 cm^2, a tree height of about 3.7 m and an average fractional cover of 35% (Rallo & Provenzano, 2013). During the investigation period, Leaf Area Index (LAI), measured with a LAI-2000 plant analyser (LiCor Biosciences Inc., Lincoln, NE, USA), was about 2.2 $m^2\ m^{-2}$ and 1.2 $m^2\ m^{-2}$ at plant and canopy level, respectively.

According to USDA classification, soil in the farm is silty clay loam. Olive trees are irrigated by a trickle irrigation system, with four 8 l h^{-1} emitters per plant. The climate in the area is typically Mediterranean, with moderate rainfall during autumn and winter, high air temperature and scarce precipitation during summer. Five plants were selected in the farm and subjected to two different irrigation regimes: three of them followed the typical scheduling practised by the farmers of the region (ordinary scheduling with watering on July 14, 19 and on August 9 and 26), whereas the other two plants were irrigated fully, with a grid of emitters covering an area of 8 m × 10 m around the two trees, applying about 5 mm of irrigation water every three days. In this way, soil water content in the root zone was maintained approximately at field capacity ($\theta_{fc} = 0.32$ $cm^3\ cm^{-3}$) during the entire investigation period. The experimental set-up therefore created substantial differences in soil/plant water status and allowed collection of a set of leaf and canopy spectral measurements under a wide range of leaf water potentials.

In the selected plants, temporal and spatial variability of soil water contents was monitored at several depths, ranging between 10 and 85 cm, using a Diviner2000 capacitance probe (Sentek Technologies, Adelaide, Australia). A total of 5 and 3 access tubes were installed around the trees subjected to the ordinary and full irrigation respectively.

Measurements were made from June to August 2011. During the experimental period, in order to estimate the atmospheric evaporative demand, a set of standard climatic data (air temperature and relative humidity, solar radiation, wind speed, etc.) were acquired by a meteorological station located approximately 500 m apart from the study area.

2.2. Spectral and physiological measurements

Leaf and canopy reflectance were monitored with an ASD FieldSpec Pro spectroradiometer (Analytical Spectral Device, Inc.), covering VIS to SWIR wavelengths (350–2500 nm), characterised by an internal field of view (IFOW) of 25° and sampling intervals of 1.4 nm and 2.0 nm, respectively in regions between 350–1000 nm and 1000–2500 nm.

At tree canopy level, spectral signatures were acquired with the sensor placed over an aluminium mast mounted on a horizontal arm. The sensor, maintained at a distance of 1 m above the canopy, was directed vertically downward (nadir view), in order to capture a portion of full canopy, extending over about 0.12 m^2.

All the spectral measurements were made around 11.30 or 14.30 local time (GMT + 2), in the absence of clouds, under a solar angle from the zenith always less than 45°, from the end of June to the end of August (June, 27, July 5, 11 and 19, August 2, 16, 23 and 30). Each measurement was obtained by averaging three scans, giving a total of 39 spectra acquired during the entire period.

The measurement targets were pre-selected opportunely and chosen in the external side of the tree canopy in order to avoid the disturbance due to the tree branches and to consider different leaves. Preliminary field measurements verified that there was only a limited effect on the spectral response from small differences in angular configuration (MacArthur, MacLellan, & Malthus, 2012) and from the background observed through the canopy.

At leaf level, the measurements required the use of the ASD Contact Probe and Leaf clip (Analytical Spectral Device, Inc.), specifically designed to collect contact spectra on live vegetation. Using these two accessories, leaf spectra were acquired on the adaxial surface of leaves chosen on a detached one-year-old shoot, between predawn and 14.30, before and after acquisitions at canopy levels. Because the instrument was handheld and independent of the solar light source, a larger number of spectra (total 162) were collected.

Before each acquisition at both canopy and leaf levels, the reflectance of a white standard panel (Spectralon) was measured. The percentage of canopy or leaf reflectance was then obtained by dividing the sample spectrum by the white reference spectrum and this was automatically provided in output by the instrument. The Savitzky and Golay (1964) procedure was applied as pre-treatment to smoothing reflectance spectral measurements. The Savitzky–Golay filter uses a local polynomial least squares fit within a moving window, in order to assign a smoothed value to each raw reflectance data point. A second order polynomial and a moving window of 15 points were adopted; due to the observed noise, reflectance values at the edge of spectral regions (wavelengths <450 nm and >2400 nm) were not used. Furthermore, at canopy level, the spectral regions commonly affected by atmospheric noise, between 1350–1420 nm and 1800–2000 nm, were not considered.

Immediately after each spectral measurement, leaf water potential was measured on the same trees with a Scholander pressure chamber (Model 600, PMS Instruments Co., Albany, USA). According to the procedure suggested by Turner (1988), the one-year-old shoot was bagged in plastic bags and cut with a razor blade before being placed in the pressure chamber. For each tree, two measurements of leaf water potential were made on each occasion.

2.3. Selection of vegetation indices

A preliminary assessment of the most widely investigated vegetation indices, VIs, was carried out in order to select those that have already been recognised as good descriptors of crop water status (Sims & Gamon, 2002; Sha & Yu, 2008).

The two most common type of VIs, i.e. the Normalized Difference Spectral Index (NDSI) and Simple Ratio Index (SRIs), combine the reflectances, R_i, of two bands, using the following expressions:

$$\mathrm{NDSI}_{(x,y)} = \frac{R_x - R_y}{R_x + R_y} \quad (1)$$

$$\mathrm{SRI}_{(x,y)} = \frac{R_x}{R_y} \quad (2)$$

where x and y indicate the so-called "centre-band", corresponding to the central wavelength of each considered band.

As observed in the literature (Huete, Jackson, & Post, 1985; Qi, Moran, Cabot, & Dedieu, 1995), the normalisation used for NDSIs is useful to reduce noise due to atmosphere, as well as to remove the systematic changes of reflectance due to other sources.

SRI indices were originally developed (Jackson & Huete, 1991) to estimate chlorophyll and anthocyanin contents on the basis of reflectance in the visible domain (350–700 nm). However, further studies (Penuelas, Filella, & Sweeano, 1996; Tian et al., 2001) demonstrated that, by combining near-infrared and infrared reflectances, SRIs can be used to assess the interactions between crop water status and other physiological variables.

In this study, a set of different NDSI and SRI families were selected. Definitions, formulae and references are summarised in Table 1 in which, for each considered band, the specific central wavelengths are those indicated in the original formulation proposed.

In this study, NDSIs and SRIs were optimised using the available data-set containing reflectance measurements and contextual leaf water potentials. Particularly, the "optimal" indices were derived after selecting the most appropriate wavelengths, x and y, for Eqs. (1) and (2). For each spectrum and in each considered band, all the possible combinations of 1 nm wavelength were used in Eqs. (1) and (2) to obtain a matrix [x,y] of corresponding VIs. The ranges 520–570 nm for green, 571–700 nm for red, 701–950 nm for NIR and finally 951–2400 nm for SWIR bands were selected. In this way, for each examined index, a set of n-matrices were obtained considering all the n-measurements acquired at different time-steps. Finally, the optimal index was deduced according to the maximum determination coefficient, R^2, of all the linear regressions between the vectors $[n,1]$ of each x,y wavelength combination and the vector $[n,1]$ containing the LWP values. This procedure was implemented on Matlab 10.0 (Mathworks, USA).

2.4. Multivariate statistical approach

As discussed in the introduction, the availability of canopy and/or leaf reflectance measurements at high spectral resolution also allows multivariate statistical analysis of the

Table 1 – Families of spectral indices used in the study.

Normalized Difference Spectral Indices, NDSI			Simple Ratio Indices, SRI		
Definition	Bands used and formula	Reference	Definition	Bands used and formula	Reference
Normalized Difference Vegetation Index	$\mathrm{NDVI} = \frac{\mathrm{NIR}-\mathrm{RED}}{\mathrm{NIR}+\mathrm{RED}} = \frac{R_{800}-R_{680}}{R_{800}+R_{680}}$	(Rouse, Haas, Deering, & Sehell, 1974)	Simple Ratio Water Index	$\mathrm{SRWI} = \frac{\mathrm{RED}}{\mathrm{IR}} = \frac{R_{680}}{R_{1240}}$	(Zarco-Tejada, Rueda, & Ustin, 2003)
Green Normalized Difference Vegetation Index	$\mathrm{GNDVI} = \frac{\mathrm{NIR}-\mathrm{GREEN}}{\mathrm{NIR}+\mathrm{GREEN}} = \frac{R_{800}-R_{550}}{R_{800}+R_{550}}$	(Gitelson and Merzlyak, 1994)	Green Index	$\mathrm{GI} = \frac{\mathrm{GREEN}}{\mathrm{RED}} = \frac{R_{550}}{R_{680}}$	(Chamard et al. 1991)
Normalized Difference Greenness Vegetation Index	$\mathrm{NDGI} = \frac{\mathrm{GREEN}-\mathrm{RED}}{\mathrm{GREEN}+\mathrm{RED}} = \frac{R_{550}-R_{680}}{R_{550}+R_{680}}$	(Chamard et al. 1991)	Water Index	$\mathrm{WI} = \frac{\mathrm{RED}}{\mathrm{NIR}} = \frac{R_{680}}{R_{858}}$	(Peñuelas et al., 1993)
Normalized Difference Water Index	$\mathrm{NDWI} = \frac{\mathrm{NIR}-\mathrm{IR}}{\mathrm{NIR}+\mathrm{IR}} = \frac{R_{858}-R_{1240}}{R_{858}+R_{1240}}$	(Gao, 1996)	Moisture Stress Index	$\mathrm{MSI} = \frac{\mathrm{NIR}}{\mathrm{IR}} = \frac{R_{858}}{R_{1240}}$	(Hunt & Rock, 1989)

relationship with crop water status. Particularly, the Partial Least Squares Regression (PLSR) is a standard multivariate statistical technique for spectral calibration and for prediction of material properties (Martens and Naes, 1989, p. 419), using the whole information included in spectral measurements. Several studies have successfully demonstrated the effectiveness of spectral measurements and PLSR to predict various biophysical crop parameters (Hansen & Schjoerring, 2003). PLSR is a standard bilinear regression method, using a compressed dataset obtained by reducing the large number of measured collinear spectral variables (in our case the high number of reflectance values for each measured spectra) to a few non-correlated "latent variables". The compression of data is performed using Principal Components (PCs) analysis of measured spectral variables (Ehsani, Upadhyaya, Slaughter, Shafii, & Pelletier, 1999). In other words, the PCs represent the relevant structural information included in the reflectance measurements and allow prediction of the dependent variable. The basic PLSR algorithm, described in Esbensen (2000, 598 pp.), is implemented in Unscrambler 9.7 software (Camo, USA). PLSR analysis was performed on the mean-centred 1st derivative reflectance measurements, in order to amplify the "peakedness" of spectra due to the absorption features. The PLSR technique was applied using the "leave one-out" cross-validation method (Clarke, Fokoue, & Zhang, 2009, p. 798) over the entire set of canopy and leaf level measurements.

3. Results and discussion

3.1. *Physiological and hydrological measurements*

For the investigated period, Table 2 summarises the average values and the corresponding variability of leaf water potential, LWP (MPa) and soil water contents, θ ($m^3\ m^{-3}$) measured for plants under ordinary and full irrigation; Table 2 also shows the daily reference evapotranspiration, ET_0 ($mm\ d^{-1}$), as well as the kind of acquired spectra (leaf and/or canopy). During each measurement day, leaf water potentials were obtained by separately averaging the values acquired from the plants under ordinary irrigation, LWP_o (MPa), and from those subject to full irrigation, LWP_w (MPa). Similarly, the corresponding soil water contents were obtained by averaging the values measured in the root zone (15–70 cm), for a total of 30 measurements around the plants under ordinary irrigation, θ_o ($m^3\ m^{-3}$), and 18 measurements for the plants subject to full irrigation, θ_w ($m^3\ m^{-3}$). Daily reference evapotranspiration, ET_0 ($mm\ d^{-1}$), was computed on the basis of FAO-56 procedure (Allen, Pereira, Raes, & Smith, 1998, p. 326), using the measured meteorological variables.

As a consequence of different irrigation management, average soil water contents were significantly different for the two treatments, being greater for the plants subjected to full irrigation (Fig. 1a). Moreover, for plants under full irrigation the average soil water content, θ_w, was generally around the soil field capacity, without any significant variability in the root zone during the investigated period. By contrast, for plants under ordinary scheduling, the temporal trend of average soil water content, θ_o, was influenced by irrigation (Fig. 1a), with an evident drying period from July 19th (second

Table 2 – Summary of main experimental data.

Date	Leaf water potential under ordinary irrigation, LWP_o (MPa)			Leaf water potential under full irrigation, LWP_w (MPa)			Soil water content, θ ($m^3 m^{-3}$)		ET_0 ($mm\ d^{-1}$)	Kind of spectral data
	6.30 a.m.	11.30 a.m.	14.30 p.m.	6.30 a.m.	11.30 a.m.	14.30 p.m.	θ_o	θ_w		
June, 27	−0.54 (0.16)[a]	−1.81 (0.21)	−2.13 (0.12)	−0.48 (0.22)	−1.93 (0.02)	−2.29 (0.05)	–	–	6.3	Leaf/Canopy
July, 05	−0.71 (0.22)	−1.07 (0.36)	−2.38 (0.07)	−0.70 (0.30)	−0.45 (0.16)	−2.23 (0.02)	–	–	5.1	Leaf
July, 11	−0.92 (0.14)	−2.29 (0.15)	2.37 (0.04)	−0.38 (0.09)	−0.75 (0.47)	−2.30 (0.01)	–	–	5.6	Leaf/Canopy
July, 13	–	–	–	–	–	–	0.22 (0.13)[a]	0.33 (0.02)	5.6	–
July, 19	−0.93 (0.39)	−2.65 (0.08)	−2.52 (0.12)	−0.33 (0.11)	−1.93 (0.34)	−2.35 (0.03)	–	–	5.4	Leaf/Canopy
July, 21	–	–	–	–	–	–	0.25 (0.19)	0.31 (0.02)	5.3	–
July, 27	–	–	–	–	–	–	0.24 (0.23)	0.32 (0.01)	4.5	–
Aug., 02	−1.25 (0.50)	−2.66 (0.12)	−2.86 (0.08)	−0.34 (0.04)	−1.75 (0.04)	−2.03 (0.05)	0.18 (0.30)	0.29 (0.05)	5.4	Leaf/Canopy
Aug., 09	–	–	–	–	–	–	0.15 (0.33)	0.31 (0.02)	4.8	–
Aug.,16	−0.89 (0.32)	−2.63 (0.14)	−2.65 (0.14)	−0.35 (0.12)	−2.33 (0.09)	−2.34 (0.15)	0.24 (0.27)	0.33 (0.01)	5.3	Leaf
Aug., 23	−1.89 (0.23)	−3.39 (0.12)	−3.52 (0.11)	−0.30 (–)	−2.25 (0.19)	−2.42 (0.04)	0.15 (0.36)	0.26 (0.08)	5.0	Leaf/Canopy
Aug., 30	−0.90 (0.38)	−2.71 (0.14)	−3.16 (0.11)	−0.42 (0.08)	−2.25 (0.06)	−2.55 (0.03)	0.23 (0.30)	0.32 (0.02)	4.4	Leaf/Canopy

[a] Coefficients of variation.

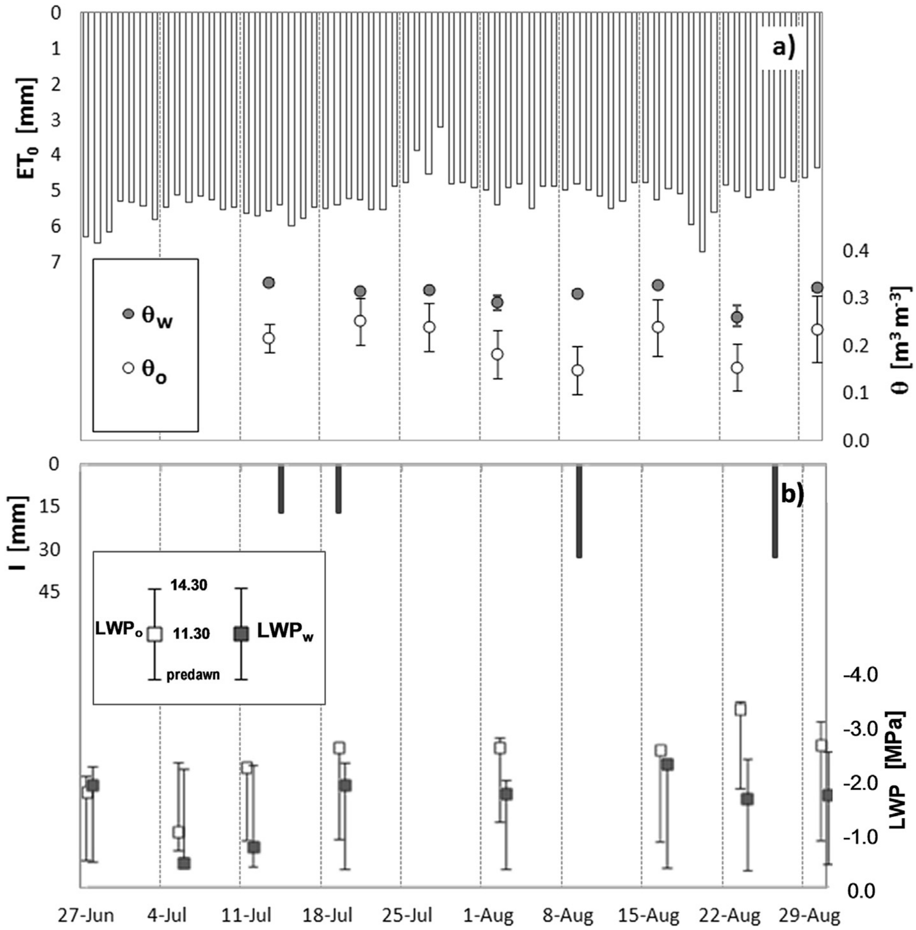

Fig. 1 – Temporal dynamic of observed variables during the experimental period. Upper graph (a) shows reference evapotranspiration, ET_0, and average soil water contents, θ_0 e θ_w measured on plants subjected to ordinary and full irrigation; line bars indicate standard deviation of θ. Lower graph (b) shows the ordinary irrigation depths, I (mm) and, for both treatments, the average leaf water potential, LWP measured at 11.30. Line bars indicate the variability of LWP between predawn (lower values) and 14.30 (upper values).

watering) to August 9th (third watering). For these plants, the variability of soil water content in the root zone was about 5%, due to the localised system used for irrigation.

The corresponding changes of measured leaf water potential were more complex. As can be observed in Fig. 1b, predawn leaf water potentials were quite stable and generally around −0.4 and −1.0 MPa, respectively, for full and ordinary irrigation. Leaf water potentials measured at 11.30 decreased during the first 20 days of July, from −0.5 to −2.4 MPa and from −1.1 to −3.4 MPa, for full and ordinary irrigation respectively.

Only for the first two measurements in July (4th and 11th) were LWPs measured at 11.30 on fully irrigated trees similar to the corresponding predawn values. This could be related to a combined effect of soil water status and atmospheric water demand (ET_0); in fact, it can be noticed that in the period between July 4th and 11th, if soil water status assumes the highest values, the atmospheric demand is moderate.

It is interesting to note that after the first ten days of July, for ordinary irrigation, leaf water potentials measured at 11.30 were equal to or slightly higher than those measured at 14.30, whereas for full irrigation, the corresponding values were in general much higher than those measured at 14.30. This circumstance reflects the typical behaviour of drought tolerant plants like olives that, during periods of high atmospheric demand, reduce transpiration by closing their stomata (Saie, Zamani, & Talaie, 2008).

3.2. *Spectral measurements*

All pre-treated spectral measurements used in this study are plotted in Fig. 2. For both spectral measurements (leaf and canopy levels), there were jumps in raw data at the transition wavelengths between the 3 ASD detectors of the spectroradiometer (around 1000 and 1800 nm). Therefore, to minimise noise in the spectral analysis, these wavelengths were removed from the measured data. Moreover, at tree canopy level, the missing reflectances corresponding to wavelengths around 1400 nm and in the range from 1800 nm to 2000 nm are due to atmospheric noise.

Like any other green vegetation spectrum, Fig. 2a, and b show high reflectance in the NIR and low reflectance in the VIS

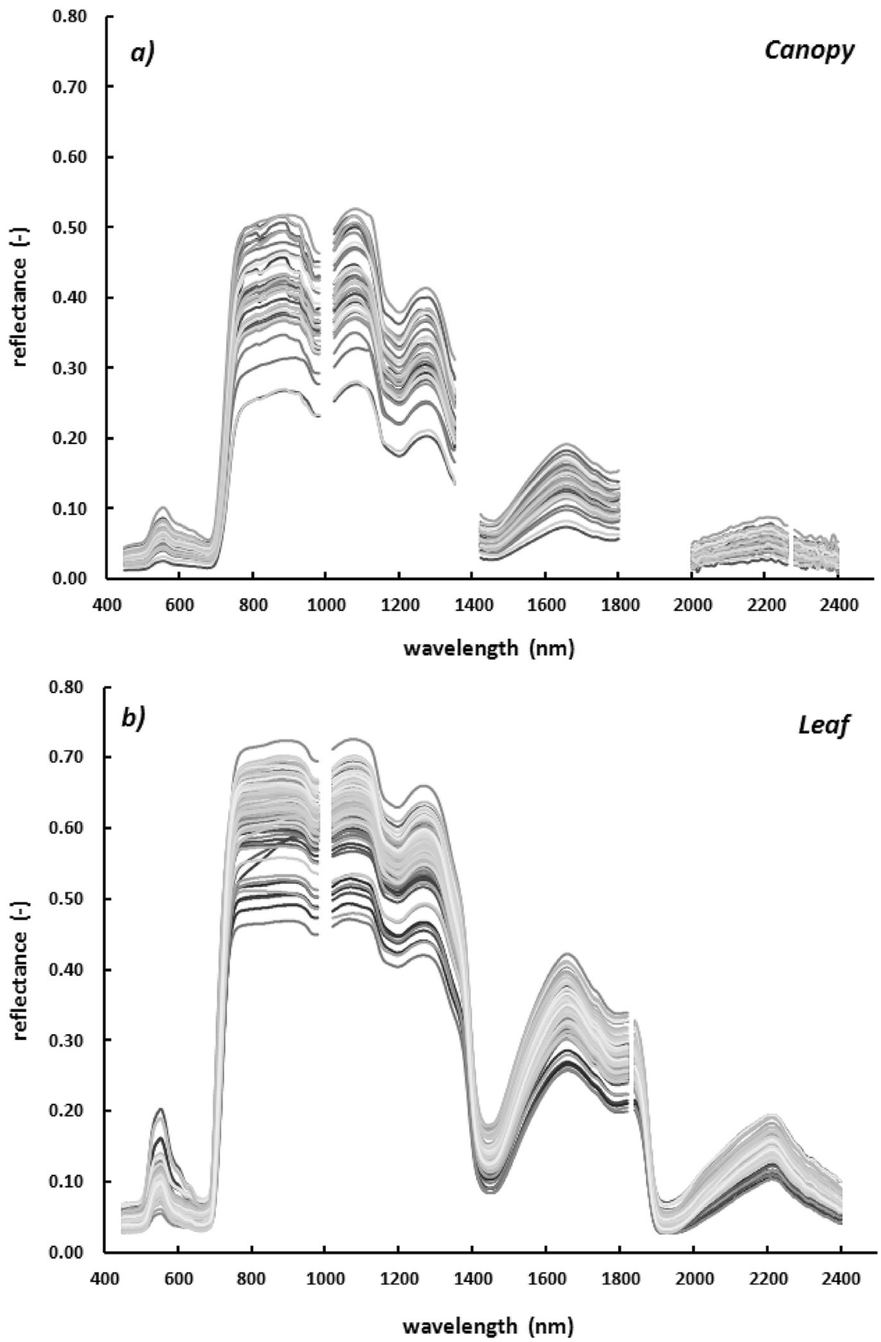

Fig. 2 – Measured spectra at (a) canopy and (b) leaf levels.

regions, with a typical peak at 550 nm. Other typical spectral responses can be observed in the SWIR region, where at leaf scale, absorbance bands near 1450 and 1900 nm (Fig. 2b), could be related to the leaf water content. Differences between spectral signatures measured at leaf and tree canopy level are a consequence of the measurement target; in fact, at canopy level the target includes a spatial distribution of shadowed and well-lit leaves with different angular distributions, whereas at leaf level the reflectances were always measured on the adaxial surface.

All data were used to optimise VIs, whereas a random separation into two sub-databases, i.e. calibration (65% of observations) and validation (35% of observations), was considered for the cross-validation of the relationships between optimised VIs and leaf water potential. The leave-one-out technique was used for the cross-validation and the procedure was repeated 10 times in order to analyse and compare all the statistical parameters.

3.3. *Optimisation of Vegetation Indices for estimating leaf water potential*

Figure 3 shows, at tree canopy level and for all the considered indices, the contour maps of R^2, allowing the "hot spots"

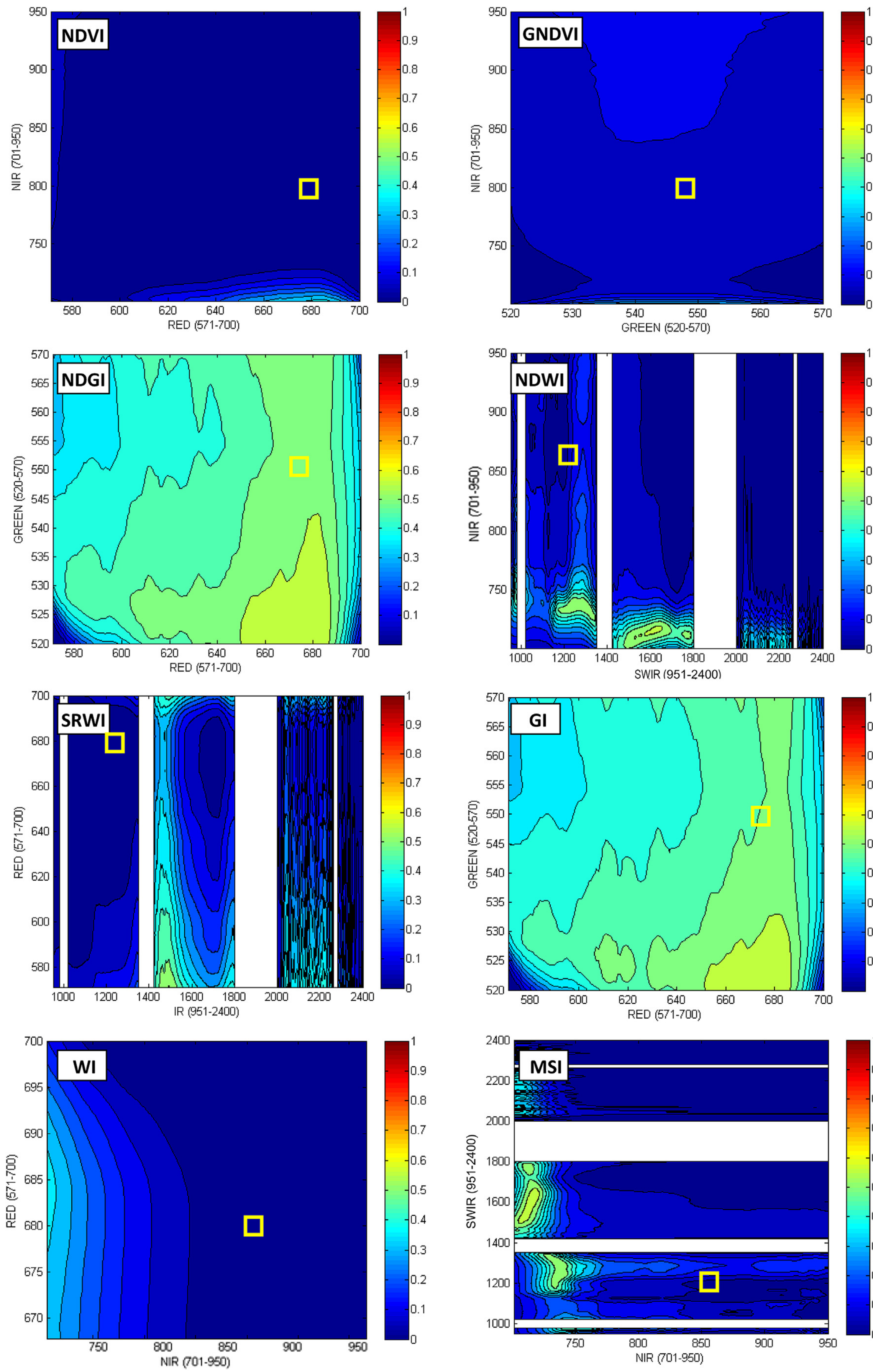

Fig. 3 – Contour maps of R^2 between measured leaf water potentials and all possible tree canopy level VIs optimised using all combinations of wavelengths centre-bands. Yellow box indicates R^2 calculated with the original wavelengths combination.

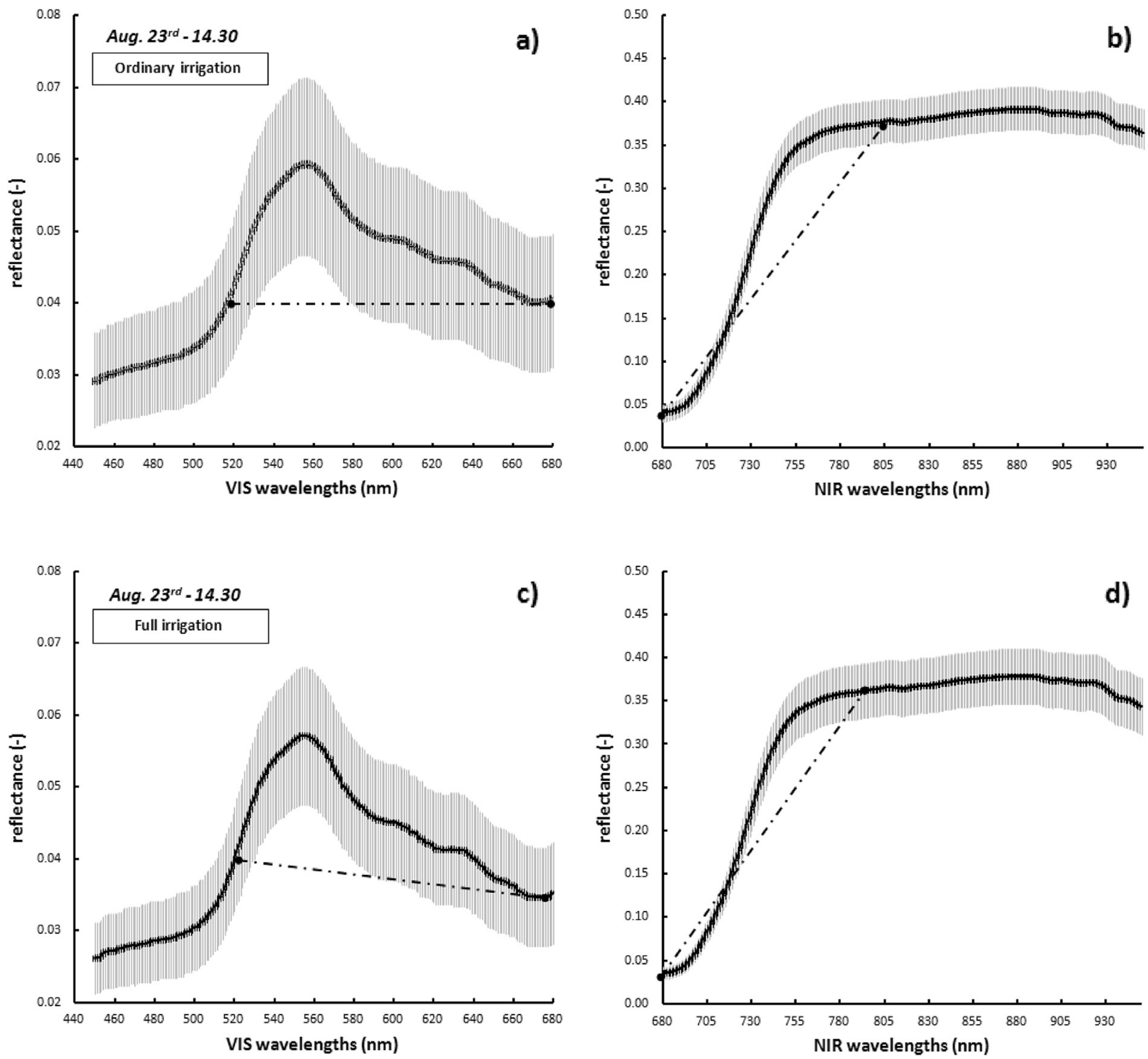

Fig. 4 – VIS–NIR spectral measurements at canopy level on plants under ordinary (a,b) and full (c,d) irrigation, acquired during a water stress day. Grey bars indicate the variability of spectra (min and max) measured in the investigated plants. For plants under ordinary and full irrigation the average leaf water potential resulted −3.4 and −2.4 MPa, NDGI was equal to 0.021 and 0.062 whereas NDVI equal to 0.80 and 0.82, respectively. The slopes of dotted lines highlight the higher sensitivity of optimised NDGI compared to NDVI.

representing the best combination of optimised wavelengths to be identified. In the figures yellow boxes indicate the original wavelength combination given in Table 1.

As can be observed in Fig. 3, none of standard VIs gave a satisfactory description of leaf water potential. The poor correlations between the standard indices (e.g. NDVI) and LWPs could be explained by considering that olive is a typical drought resistant crop. Leaf tissues are constituted of sclerophyll, which can only be damaged in presence of high and persistent water stress conditions. However, the common VIs were formulated for typical vegetation tissues constituted of chloroplast, which can be damaged also by normal stress conditions, generating the typical decrease in NIR reflectance and in standard indices such NDVI.

However, for some families of indices, a better performance can be found when wavelengths are shifted to the specific hot spot. For example, prediction of LWP from NDVI can be improved if the NIR band is centred inside the "red-edge" region, i.e. around 705 nm (Fig. 3, upper left panel). A similar result has been observed by other authors (Gitelson & Merzlyak, 1994; Sims & Gamon, 2002), who showed that reflectance measurements in the "red-edge" spectral region (680–740 nm) allow the concentrations of various pigments related to leaf water status to be described. However, this kind of procedure can only be applied when data with high spectral resolution are available.

At canopy level, the best descriptors of leaf water potential were the optimised Normalized Difference Greenness

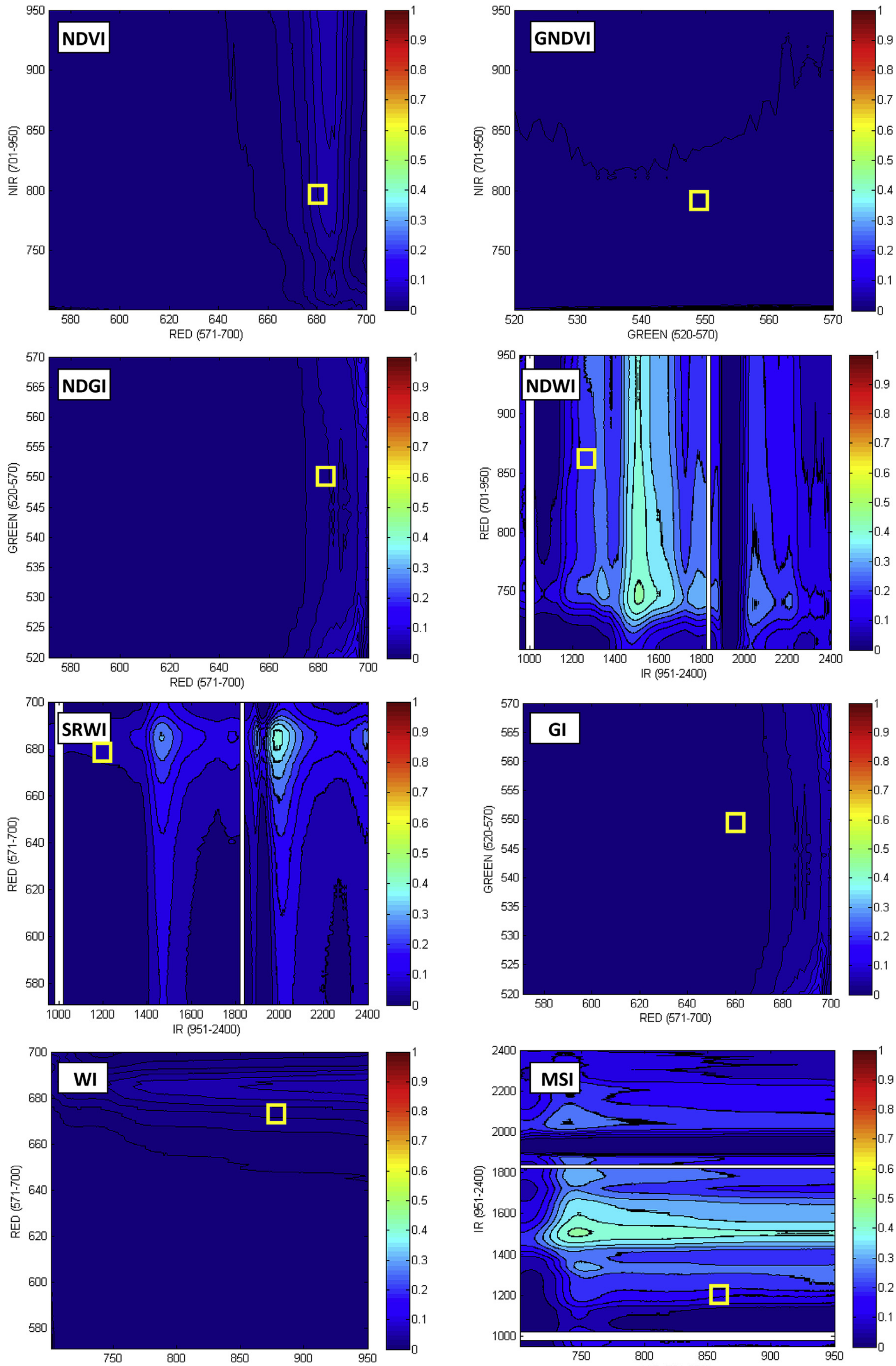

Fig. 5 – Contour maps of R^2 between measured leaf water potentials and all possible leaf scale VIs optimised using all combinations of wavelengths centre-bands. Yellow box indicates R^2 calculated with the original wavelengths combination.

Table 3 – Correlation analysis results between VIs derived from canopy scale spectra and LWP.

Vegetation Indices	Model's parameters		Calibration data ($n = 26$)				Validation data ($n = 13$)			
	Slope (a)	Intercept (b)	(R^2)	RMSE	SE	P	(R^2)	RMSE	SE	P
NDVI	16.32 (2.67)[a]	−6.96 (0.77)	0.36 (0.09)	0.44 (0.02)	0.44 (0.03)	<0.01	0.36 (0.16)	0.45 (0.05)	0.44 (0.06)	<0.05
GNDVI	−19.88 (0.78)	−1.25 (0.07)	0.41 (0.07)	0.45 (0.04)	0.43 (0.05)	<0.01	0.22 (0.07)	0.50 (0.08)	0.51 (0.08)	>0.05
NDGI	17.30 (1.70)	−3.63 (0.14)	0.62 (0.07)	0.35 (0.03)	0.36 (0.03)	<0.001	0.57 (0.09)	0.37 (0.08)	0.35 (0.06)	<0.01
NDWI	12.58 (2.43)	−3.11 (0.11)	0.63 (0.12)	0.33 (0.04)	0.34 (0.04)	<0.001	0.44 (0.24)	0.46 (0.09)	0.47 (0.09)	<0.05
SRWI	3.41 (0.56)	−6.38 (0.65)	0.50 (0.10)	0.37 (0.03)	0.38 (0.03)	<0.001	0.45 (0.12)	0.46 (0.05)	0.47 (0.06)	<0.05
GI	7.82 (0.90)	−11.42 (1.05)	0.59 (0.07)	0.36 (0.03)	0.36 (0.03)	<0.001	0.53 (0.08)	0.39 (0.04)	0.38 (0.05)	<0.01
WI	−12.79 (1.37)	4.46 (0.68)	0.38 (0.07)	0.44 (0.03)	0.45 (0.03)	<0.001	0.42 (0.20)	0.46 (0.04)	0.43 (0.08)	<0.05
MSI	−6.34 (0.62)	3.02 (0.52)	0.62 (0.06)	0.35 (0.02)	0.35 (0.02)	<0.001	0.48 (0.11)	0.41 (0.05)	0.39 (0.04)	<0.01

[a] Standard deviation.

Vegetation Index (NDGI), Green Index (GI), Normalized Difference Water Index (NDWI) and Moisture Spectral Index (MSI). Compared to the original definitions, the first two indices (only using VIS region, i.e., red and green bands) required a green band centred around 525 nm, instead of 550 nm. Despite the small correction of the wavelength in the green, the good performance of these two indices might be ascribed to a phenomenon known as paraheliotropism (Natali, Bignami, Cammili, & Muganu, 1999), where there is a change in leaf inclination to avoid direct solar radiation in presence of high atmospheric demand. According to this process, as observed in the literature (Baldini, Facini, Nerozzi, Rossi, & Rotondi, 1997; Levizou, Drilias, Psaras, & Manetas, 2005), there is an increase in the presentation of abaxial leaf surfaces and consequently higher reflectance values in green compared to red band occurs, leading to higher NDGI and GI values. Moreover, as observed by Levizou et al. (2005), the abaxial surface of olive leaves is covered by trichomes, which lead to a reflectance in the VIS region higher than for the adaxial surface. In order to verify this statement, spectral signatures acquired over ordinary irrigated and fully irrigated trees were compared for the driest day of the period (August 23). Fig. 4a, d shows the signatures in VIS and NIR acquired at canopy level for trees under ordinary and full irrigation; average values of NDGI, standard NDVI, and LWPs, are also indicated. As can be observed, spectral signatures of plants under ordinary irrigation, in the VIS region, are characterised by higher reflectances, whereas in the NIR region values of reflectance are similar. Particularly, observing Fig. 4a and c, it can be noticed that the value of NDGI obtained by using the optimised wavelengths (520 and 680 nm), is lower for trees under ordinary irrigation (0.021), if compared to the fully irrigated trees (0.062). Even the slopes of dotted lines in the VIS region (Fig. 4a and c) demonstrate the sensitivity of optimised NDGI to crop water status. By contrast, in the NIR region, Fig. 4b and d show similar values of NDVI (0.80 and 0.82), as confirmed by the slope of the dotted lines, evidencing the slight sensitivity of this index to crop water status. However, further investigation is necessary to test the robustness of these results.

Using spectral data at leaf level, none of standard definitions of VIs gave a satisfactory description of LWP in terms of R^2 (Fig. 5). The best descriptors were obtained optimising NDWI and MSI. For these two indices, it was necessary to shift the original wavelengths from 858 nm to 715 nm in NIR and from 1215 nm to around 1650 nm in SWIR (Fig. 5). The reasonable performance of these indices is possibly a consequence of the typical SWIR water absorption features (centred around 1500 nm, 1800 nm and 1900 nm). A similar result has also been obtained by Tian et al. (2001), who indicated that leaf reflectance spectra, in the 1650–1850 nm region, are influenced by their water content.

Even at leaf level, the amplitude of hot spots (Fig. 5), identifying the optimal wavelengths in NIR and SWIR regions, suggests that the improved indices can be applied using broader bands of about 30 and 50 nm, respectively. Reflectance in SWIR region can be obtained by using contact sensors with the advantage of avoiding the noise generated by atmospheric water vapour, though this would limit the applicability of the methodology from remote sensors.

Tables 3 and 4 show the results of the cross-correlation analysis between the optimised indices and LWPs at canopy and leaf levels, respectively. In addition to the determination coefficient (R^2), the overall accuracy estimation was evaluated by means of the Root Mean Square Error (RMSE) and the Standard Error (SE):

$$\mathrm{RMSE} = \sqrt{\left(\frac{1}{N}\sum_{i=1}^{N}(M_i - O_i)^2\right)} \tag{3}$$

$$\mathrm{SE} = \sigma(M_i - O_i) \tag{4}$$

where N is the number of measurements, M_i is the value of the i-th predicted variable, O_i is the value of the i-th measured variable, and σ indicates the standard deviation operator.

For each index, Tables 3 and 4 also show the standard deviation (average of ten repetitions), the regression parameters (slope, intercept), and the statistical significance, P, of the regressions between indices and leaf water potential. Assuming that for practical applications, an error of estimation on LWP equal to the standard deviation of measurements is acceptable, values of 0.56 MPa and 0.97 MPa were assumed as threshold errors at tree canopy and leaf level respectively. The different thresholds assumed for the two types of spectral measurement is a consequence of the different number of each measurement in the database; in fact, at leaf level, measured LWPs included predawn values, so resulting in a wider range (−0.3 to −4.0 MPa) compared to the canopy level (−1.5 to −4.0 MPa).

Table 4 – Correlation analysis results between VIs derived from leaf scale spectra and LWP.

Vegetation Indices	Model's parameters		Calibration data ($n = 98$)				Validation data ($n = 64$)			
	Slope (a)	Intercept (b)	(R^2)	RMSE	SE	P	(R^2)	RMSE	SE	P
NDVI	−11.09 (1.91)[a]	7.46 (1.62)	0.09 (0.03)	0.93 (0.03)	0.94 (0.03)	<0.01	0.05 (0.04)	0.95 (0.05)	0.95 (0.04)	>0.05
GNDVI	−2.45 (2.26)	−0.04 (1.71)	0.02 (0.02)	0.98 (0.02)	0.98 (0.02)	>0.05	0.02 (0.01)	0.96 (0.06)	0.96 (0.05)	>0.05
NDGI	16.79 (1.33)	−2.70 (0.07)	0.15 (0.03)	0.89 (0.03)	0.90 (0.03)	<0.001	0.12 (0.04)	0.93 (0.04)	0.92 (0.04)	<0.01
NDWI	18.85 (1.66)	−12.06 (0.87)	0.47 (0.03)	0.70 (0.03)	0.70 (0.03)	<0.001	0.45 (0.05)	0.75 (0.05)	0.74 (0.04)	<0.001
SRWI	4.86 (0.14)	−6.51 (0.14)	0.42 (0.02)	0.74 (0.02)	0.74 (0.02)	<0.001	0.41 (0.04)	0.75 (0.03)	0.74 (0.03)	<0.01
GI	−8.69 (1.22)	6.04 (1.13)	0.13 (0.04)	0.89 (0.04)	0.89 (0.04)	<0.001	0.15 (0.05)	0.93 (0.06)	0.93 (0.06)	<0.01
WI	18.07 (4.51)	−3.42 (0.38)	0.09 (0.05)	0.91 (0.03)	0.91 (0.03)	<0.01	0.06 (0.04)	0.99 (0.05)	0.99 (0.05)	<0.05
MSI	−19.36 (0.85)	4.99 (0.31)	0.47 (0.03)	0.71 (0.02)	0.72 (0.02)	<0.001	0.45 (0.05)	0.72 (0.03)	0.72 (0.03)	<0.001

[a] Standard deviation.

Assuming these thresholds, NDGI, GI, and MSI can be used, at canopy level, as predictors of LWPs, whereas NDWI and MSI are reasonable predictors of LWPs from spectral data acquired at leaf level.

In any case, though the two "green indices" at canopy level (NDGI and GI) could be influenced by external factors (e.g. paraheliotropism or trichomes), the chance to use them as predictor of LWPs is relevant, as a consequence of the wide availability of sensors using only the visible domain of the spectrum. On the other hand, MSI is directly influenced by the leaf water content and it is not affected by external factors, but its use requires spectral information that is not always available.

Analysis of data indicated in Tables 3 and 4 shows higher RMSE and SE at leaf scale compared to tree canopy scale, and this may be due to the wider range of LWPs explored at leaf scale.

For the best VIs, Figs. 6 and 7, illustrate measured LWPs as a function of the best optimised VIs (three at canopy level and two at leaf level), and comparisons between predicted and measured LWPs.

Each scatterplot shows the entire data-set, whereas the slope and intercept of the regression lines are indicated in Tables 3 and 4 for the calibration subset. All experimental data for LWP are disposed around the best fit lines, with 1:1 RMSE values similar to those of Tables 3 and 4, obtained in cross-validation.

At leaf level, the scatterplots between measured and predicted LWPs (Fig. 7b and d) confirmed higher values of RMSE compared to the canopy level. This behaviour is again related to the wider range of LWP explored at leaf scale.

3.4. *Multivariate analysis*

A statistical description of the performance of PLSR technique to predict LWPs is summarised in Tables 5 and 6, considering both the data-sets acquired at canopy and leaf levels. For each of considered spectral domain (VIS, VIS–NIR, NIR–SWIR and VIS–NIR–SWIR), the overall accuracy estimation was evaluated by means of R^2, RMSE, and SE.

According to the values of statistical indices (R^2, RMSE, SE) it is evident that PLSR gives more accurate results compared to the VI approach at for both leaf and canopy data. Figures 8 and 9 show the comparison between measured and estimates LWP using the PLSR technique combined with the "leave one-out cross validation" (Clarke et al., 2009, p. 798).

Figure 8a confirms that the visible part of spectra can explain the variability of LWPs; moreover, even using just NIR–SWIR bands (Fig. 8b), LWPs can be predicted with an accuracy similar to that obtained limiting the PLSR to the VIS domain.

At leaf scale (Fig. 9), the best prediction of LWPs requires the use of PLSR in NIR–SWIR domain.

The noteworthy results obtained by using PLSR, applied at both canopy and leaf levels, are clearly due to the advantages of using, for each region, the full spectral information and not just two wavelengths, as required by VIs approach. However, this approach requires the use of field spectroscopy techniques or hyper-spectral proximal sensing.

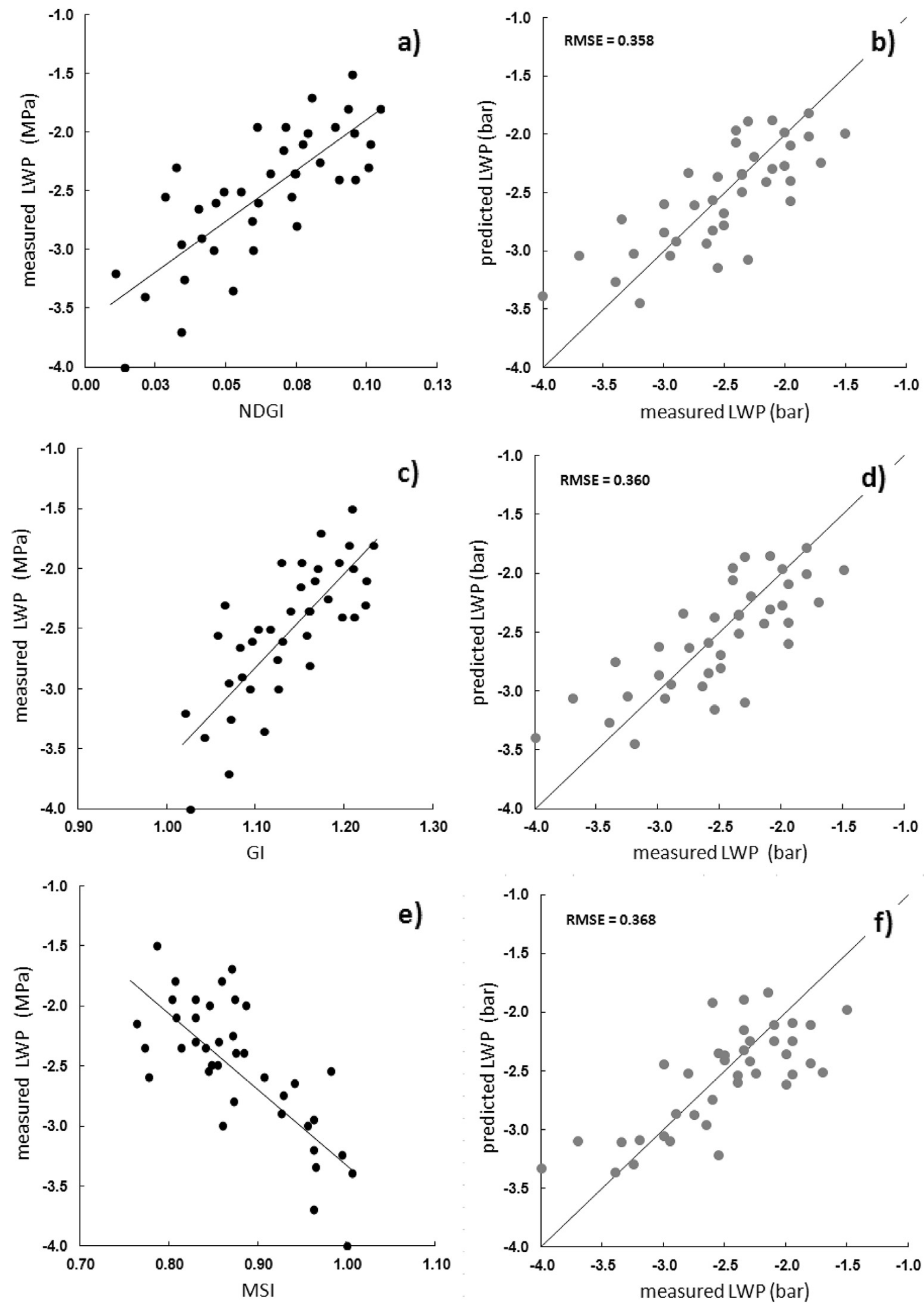

Fig. 6 – Left column: relationships between optimised spectral indices at canopy scale (NDGI, GI, MSI) and leaf water potential. Each scatterplot (black circles) shows the entire data-set, whereas the slope and intercept of regression lines are those reported in Table 3 for calibration. Right column: measured vs. predicted LWPs.

4. Conclusions

The main objective of the work was to verify how VIS–SWIR reflectance measurements at canopy and leaf levels can be used to monitor crop water status in terms of leaf water potential, for an olive grove of Sicily. Two different approaches were tested: i) optimisation and correlation analysis between a set of VIs and measured LWP and ii) Partial Least-Squares Regression method, using the full spectral information.

With the first approach, a good prediction of LWPs from canopy level reflectance data, functional to practical applications, was obtained considering two simple VIS-based

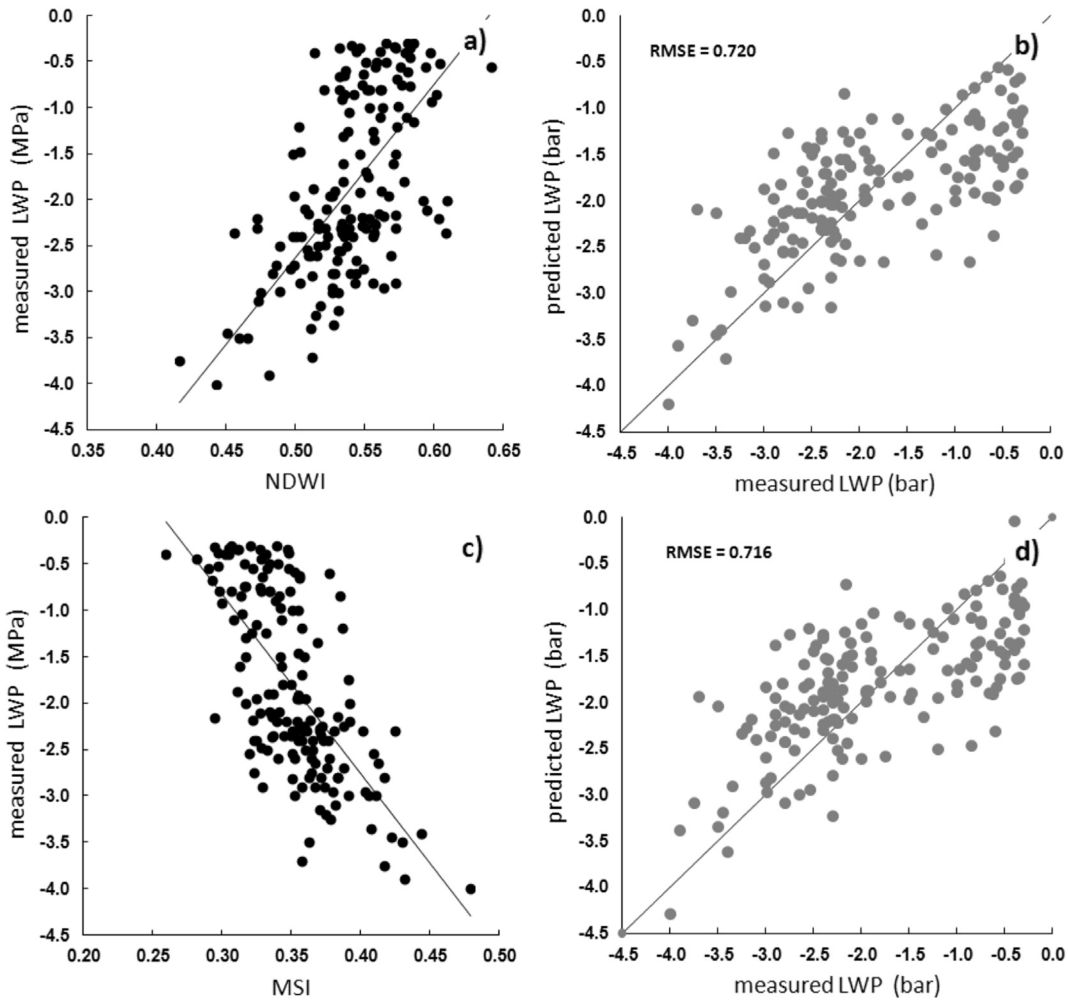

Fig. 7 – Left column: relationships between optimised spectral indices at leaf scale (NDWI and MSI) and leaf water potential. Each scatterplot (black circles) shows the entire data-set, whereas the slope and intercept of regression lines are those reported in Table 4 for calibration. Right column: measured vs. predicted LWPs.

vegetation indices, i.e. GI and NDGI, that can be easily estimated from sensors equipped with only two visible bands (green and red). However, the efficiency of prediction could only be indirectly ascribed to leaf water potential, due to the possible influence of "Paraheliotropism"; olive trees, under stress conditions, modify leaf inclination, exposing the abaxial surface, which is characterised by higher reflectance in the VIS region. However, further investigations are required to test the robustness of this statement.

When NIR and SWIR bands are available, a satisfactory prediction of LWP can be obtained by means of simple "broad-band" VIs, such as NDWI and MSI. In this case NIR and SWIR bands should be centred respectively on 715 nm, lower than the standard 858 nm, and on around 1650 nm, in place of the original 1215 nm.

At leaf level, the results showed that only optimised VIs, i.e. NDWI and MSI defined in the NIR–SWIR regions, provide a good performance at predicting LWP. For these two indices, the

Table 5 – Statistical parameters obtained from PLSR using different canopy spectral measurements as predictive variables for LWP.

Spectral regions	Calibration data ($n = 26$)			Validation data ($n = 13$)		
	(R^2)	RMSE	SE	(R^2)	RMSE	SE
VIS	0.81 (0.12)[a]	0.234 (0.09)	0.21 (0.09)	0.60 (0.06)	0.336 (0.03)	0.32 (0.04)
VIS–NIR	0.78 (0.04)	0.246 (0.01)	0.25 (0.01)	0.64 (0.10)	0.360 (0.04)	0.37 (0.04)
NIR–IR	0.80 (0.11)	0.227 (0.08)	0.23 (0.08)	0.66 (0.04)	0.326 (0.03)	0.32 (0.03)
VIS–NIR–IR	0.76 (0.08)	0.304 (0.08)	0.31 (0.08)	0.61 (0.14)	0.346 (0.08)	0.35 (0.08)

[a] Standard deviation.

Table 6 – Statistical parameters obtained from PLSR using different leaf spectral measurements as predictive variables for LWP.

Spectral regions	Calibration data ($n = 98$)			Validation data ($n = 64$)		
	(R^2)	RMSE	SE	(R^2)	RMSE	SE
VIS	0.32 (0.30)[a]	0.396 (0.232)	0.52 (0.14)	0.12 (0.07)	0.695 (0.06)	0.70 (0.05)
VIS–NIR	0.75 (0.14)	0.361 (0.16)	0.37 (0.16)	0.38 (0.06)	0.572 (0.01)	0.56 (0.01)
NIR–IR	0.83 (0.03)	0.390 (0.232)	0.29 (0.02)	0.70 (0.04)	0.391 (0.04)	0.36 (0.03)
VIS–NIR–IR	0.87 (0.08)	0.210 (0.09)	0.21 (0.09)	0.66 (0.05)	0.429 (0.03)	0.43 (0.02)

[a] Standard deviation.

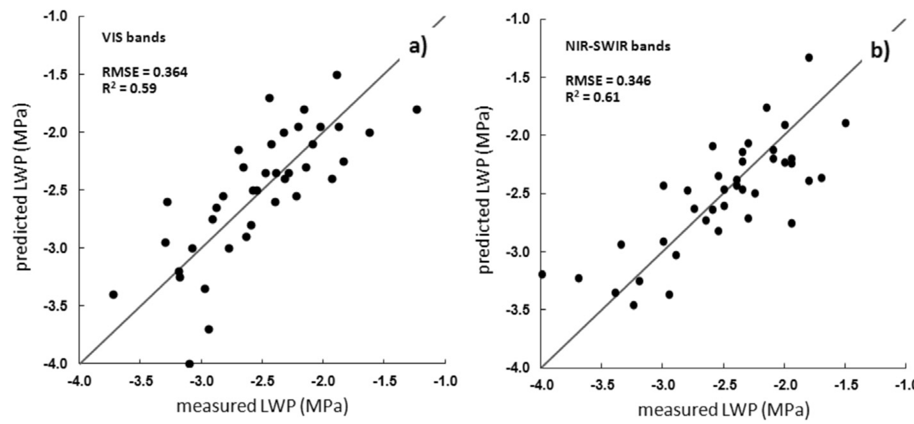

Fig. 8 – Measured vs. Predicted leaf water potential using PLSR and all bands of tree canopy level VIS (a) and NIR–SWIR (b), respectively.

optimised NIR band should be centred on 750 nm, in place of the standard 858 nm, whereas the SWIR band should be centred on a wavelength of around 1550 nm, instead of the original 1240 nm. Of course, these two indices can only be used with spectral measurements acquired with contact devices.

On the other hand, the PLSR technique provided the best predictions of LWPs at both canopy and leaf levels. The improved results are a consequence of using all the wavelengths for each spectral region and not just two wavelengths, as required by the VI approach. Therefore, it can be considered a solution only for field spectroscopy applications or for hyper-spectral proximal sensing.

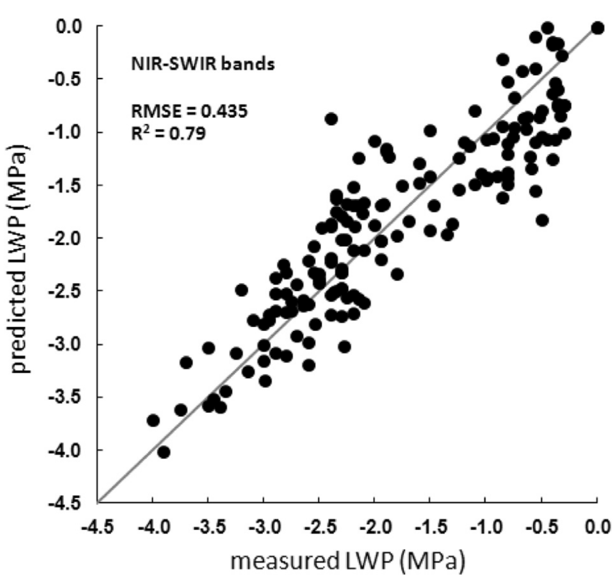

Fig. 9 – Measured vs. Predicted leaf water potential using PLSR and all bands of NIR–SWIR spectral domain at leaf level.

Finally, the study demonstrated that spectral information can be used to quantify an important biophysical parameter like leaf water potential. Depending on the specific target of the research, the spectral approach needs to be properly tuned, in order to find the most appropriate solution.

The recent technological progress in industrial production of handheld spectroradiometers and hyperspectral sensors can permit solutions for different applications. For precision farming, depending on the cost/benefit ratio, field spectroscopy with handheld devices working in VIS–NIR and SWIR regions could support crop water status monitoring for irrigation scheduling. Over large areas, the proposed approaches, combined with VIS–NIR remote sensors, could be used to monitor spatial and temporal crop parameters and to manage water resources.

Acknowledgements

The contribute to the manuscript has to be divided as following: Field collection and treatment of data were by G. Rallo and M. Minacapilli. All the Authors equally contributed to set-up the research and to write the paper. The research was co-financed from Ministero dell'Istruzione, dell'Università e della Ricerca (PRIN 2010-2011, Provenzano) (www.miur.it) and Università degli Studi di Palermo (FFR 2012). A special thank to the anonymous reviewers and to the editor in chief for the contributions aimed at improving the final quality of the manuscript.

REFERENCES

Allen, R. G., Pereira, L. S., Raes, D., & Smith, M. (1998). *Crop evapotranspiration. Guideline for computing crop water requirements.* FAO irrigation and drainage paper n. 56. Rome: Italy.

Aparicio, N., Villegas, D., Casadesus, J., Araus, J. L., & Royo, C. (2000). Spectral vegetation indices as non-destructive tools for determining durum wheat yield. *Agronomy Journal, 92*, 83–91.

Baldini, E., Facini, O., Nerozzi, F., Rossi, F., & Rotondi, A. (1997). Leaf characteristics and optical properties of different woody species. *Trees, 12*, 73–81.

Blackburn, G. A. (1998). Quantifying chlorophylls and carotenoids at leaf and canopy scales: an evaluation of some hyperspectral approaches. *Remote Sensing of Environment, 66*, 273–285.

Chamard, P., Courel, M. F., Docousso, M., Guénégou, M. C., Le Rhun, J., Levasseur, J. E., et al. (1991). Utilisation des bandes spectrales du vert et du rouge pour une meilleure évaluation des formations végétales actives. In AUPELF-UREF (Ed.), *Télédétection et Cartographie* (pp. 203–209).

Christensen, S., & Goudriaan, J. (1993). Deriving light interception and biomass from spectral reflectance ratio. *Remote Sensing of Environment, 43*, 87–95.

Clarke, B., Fokoue, E., & Zhang, H. H. (2009). *Principles and theory for data mining and machine learning*. Springer Series in Statistics. Springer.

Curran, P. J. (1989). Remote sensing of foliar chemistry. *Remote Sensing of Environment, 30*, 271–278.

Darvishzadeh, R., Skidmore, A., Schlerf, M., Atzberger, C., Corsi, F., & Cho, M. (2008). LAI and chlorophyll estimation for a heterogeneous grassland using hyperspectral measurements. *ISPRS Journal of Photogrammetry & Remote Sensing, 63*(4), 409–426.

Ehsani, M. R., Upadhyaya, S. K., Slaughter, D., Shafii, S., & Pelletier, M. (1999). A NIR technique for rapid determination of soil mineral nitrogen. *Precision Agriculture, 1*, 217–234.

Elsayed, S., Mistele, B., & Schmidhalter, U. (2011). Can changes in leaf water potential be assessed spectrally? *Functional Plant Biology, 38*(6), 523–533.

Esbensen, K. H. (2000). *Multivariate data analysis—in practice*. Corvallis: CAMO.

Gamon, J. A., & Qiu, H. (1999). Ecological applications of remote sensing at multiple scales. In F. I. Pugnaire, & F. Valladares (Eds.), *Handbook of functional plant ecology* (pp. 805–846). New York: Marcel Dekker, Inc.

Gamon, J. A., Serrano, L., & Surfus, J. S. (1997). The photochemical reflectance index: an optical indicator of photosynthetic radiation-use efficiency across species, functional types, and nutrient levels. *Oecologia, 112*, 492–501.

Gao, B. C. (1996). NDWI — a normalized difference water index for remote sensing of vegetation liquid water from space. *Remote Sensing of Environment, 58*, 257–266.

Gitelson, A., & Merzlyak, M. N. (1994). Quantitative estimation of chlorophyll-*a* using reflectance spectra: experiments with autumn chestnut and maple leaves. *Journal of Photochemistry and Photobiology, 22*, 247–252.

Goel, P. K., Prasher, S. O., Landry, J. A., Patel, R. M., & Viau, A. A. (2003). Estimation of crop biophysical parameters through airborne and field hyperspectral remote sensing. *Transactions of the ASAE, 46*(4), 1235–1246.

Hansen, P. M., & Schjoerring, J. K. (2003). Reflectance measurement of canopy biomass and nitrogen status in wheat crops using normalized difference vegetation indices and partial least squares regression. *Remote Sensing of Environment, 86*, 542–553.

Huete, A. R., Jackson, R. D., & Post, D. F. (1985). Spectral response of a plant canopy with different soil backgrounds. *Remote Sensing of Environment, 17*, 37–53.

Hunt, E. R., Jr., & Rock, B. N. (1989). Detection of changes in leaf water content using near- and middle-infrared reflectances. *Remote Sensing of Environment, 30*, 43–54.

Inoue, Y., Morinaga, S., & Shibayama, M. (1993). Non-destructive estimation of water status of intact crop leaves based on spectral reflectance measurements. *Japanese Journal of Crop Science, 62*, 462–469.

Jackson, R. D., & Huete, A. R. (1991). Interpreting vegetation indices. *Preventive Veterinary Medicine, 11*, 185–200.

Jones, H. G. (2004). Irrigation scheduling advances and pitfalls of plant-based methods. *Journal of Experimental Botany*, 55(407), 2427–2436.

Levizou, E., Drilias, P., Psaras, G. K., & Manetas, Y. (2005). Nondestructive assessment of leaf chemistry and physiology through spectral reflectance measurements may be misleading when changes in trichome density co-occur. *New Phytologist, 165*(2), 463–472.

Liang, S. (2004). Canopy reflectance modeling. *Quantitative remote sensing of land surfaces*. John Wiley & Sons, Inc.

MacArthur, A., MacLellan, C. J., & Malthus, T. G. (2012). The fields of view and directional response functions of two field spectroradiometers. *IEEE Transactions on Geoscience and Remote Sensing, 50*(10), 3892–3907.

Maccioni, A., Agat, G., & Mazzinghi, P. (2001). New vegetation indices for remote measurement of chlorophylls based on leaf directional reflectance spectra. *Journal of Photochemistry and Photobiology B Biology, 61*, 52–61.

Marino, G., Pallozzi, E., Cocozza, C., Tognetti, R., Giovannelli, A., Cantini, C., et al. (2014). Assessing gas exchange, sap flow and water relations using tree canopy spectral reflectance indices in irrigated and rainfed *Olea europea* L. *Environmental and Experimental Botany, 99*, 43–52.

Martens, H., & Naes, T. (1989). *Multivariate calibration*. Chichester: John Wiley and Sons.

Myneni, R. B., Los, S. O., & Asrar, G. (1995). Potential gross primary productivity of terrestrial vegetation from 1982–1990. *Geophysical Research Letters, 22*, 2617–2620.

Natali, S., Bignami, C., Cammili, C., & Muganu, M. (1999). Effect of water stress on leafmovement in olive cultivars. *Acta Horticulturae, 474*, 445–448.

Peñuelas, J., Filella, I., Biel, C., Serrano, L., & Savé, R. (1993). The reflectance at the 950–970 nm region as an indicator of plant water status. *International Journal of Remote Sensing, 14*, 1887–1905.

Penuelas, J., Filella, I., & Sweeano, L. (1996). Cell wall elasticity and water index (R970nm/R900nm) in wheat under different nitrogen availabilities. *International Journal of Remote Sensing, 17*, 373–382.

Penuelas, J., Gamon, J. A., Fredeen, A. L., Merino, J., & Field, C. B. (1994). Reflectance indices associated with physiological changes in nitrogen- and water-limited sunflower leaves. *Remote Sensing of Environment, 48*, 135–146.

Provenzano, G., Tarquis, A. M., & Rodriguez-Sinobas, L. (2013). Soil and irrigation sustainability practices. *Agricultural Water Management, 120*(31), 1–4.

Qi, J., Moran, M. S., Cabot, F., & Dedieu, G. (1995). Normalization of sun/view angle effects using spectral Albedo-based vegetation indexes. *Remote Sensing of Environment, 52*, 207–217.

Rallo, G., & Provenzano, G. (2013). Modelling eco-physiological response of table olive trees (*Olea europaea* L.) to soil water deficit conditions. *Agricultural Water Management, 120*, 79–88.
Rouse, J. W., Haas, R. H., Deering, D. W., & Sehell, J. A. (1974). *Monitoring the vernal advancement and retrogradation (Green wave effect) of natural vegetation*. Final Rep. RSC 1978-4. College Station: Remote Sensing Center, Texas A&M Univ..
Saie, A., Zamani, Z., & Talaie, A. R. (2008). Stomatal behavior of olive cv. zard under drought stress conditions. *Acta Horticulturae, 791*, 507–511.
Savitzky, A., & Golay, M. J. E. (1964). Smoothing and differentiation of data by simplified least squares procedures. *Analytical Chemistry, 36*, 1627–1639.
Sims, D. A., & Gamon, J. A. (2002). Relationships between leaf pigment content and spectral reflectance across a wide range of species, leaf structures and developmental stages. *Remote Sensing of Environment, 81*, 337–354.
Tian, Q., Tong, Q., Pu, R., Guo, X., & Zhao, C. (2001). Spectroscopic determination of wheat water status using 1650–1850 nm spectral absorption features. *International Journal of Remote Sensing, 22*(12), 2329–2338.
Tucker, C. J., Fung, I. Y., Keeling, C. D., & Gammon, R. H. (1986). Relationship between atmospheric CO_2 variations and a satellite-derived vegetation index. *Nature, 319*, 195–199.
Turner, N. C. (1988). Measurement of plant water status by the pressure chamber technique. *Irrigation Science, 9*, 289–308.
Sha, Z., & Yu, M. (2008). Remote sensing imagery in vegetation mapping: a review. *Journal of Plant Ecology, 1*, 9–23.
Zarco-Tejada, P. J., González-Dugo, V., Williams, L. E., Suárez, L., Berni, J. A. J., Goldhamer, D., et al. (2013). A PRI-based water stress index combining structural and chlorophyll effects: assessment using diurnal narrow-band airborne imagery and the CWSI thermal index. *Remote Sensing of Environment, 138*, 38–50.
Zarco-Tejada, P. J., Rueda, C. A., & Ustin, S. L. (2003). Water content estimation in vegetation with MODIS reflectance data and model inversion methods. *Remote Sensing of Environment, 85*, 109–124.